ISSN 2063-5346

TERNARY PHASE DIAGRAM AND RESPONSE SURFACE METHODOLOGY BASED OPTIMIZATION OF DEXIBUPROFEN NANOEMULSION

Poonam S. Patil*, Atul A. Shirkhedkar

Department of Pharmaceutical Sciences, R. C. Patel Institute of Pharmaceutical Education & Research, Shirpur, Dist-Dhule, Maharashtra, India.

Corresponding Author: Poonam S. Patil
Research Scholar, Email: poonampatil5789@gmail.com

Article History: Received: 01.02.2023 **Revised:** 07.03.2023 **Accepted:** 10.04.2023

Abstract

Background: In present work Transdermal Nanoemulsion Gel of Dexibuprofen was optimized and developed by spontaneous emulsification using a probe sonicator (d-6mm, 20KHz). Pseudoternary phase research and Response surface methodology used to find best optimized formulation. Using Central composite design formulation batches were developed at three levels with two factors based on the appropriate oil concentrations and Smix (Surfactant: Co-Surfactant). The dependent variables average droplet size, entrapment efficiency, and percent drug release for each batch were examined. All batches exhibit globule size less than 200nm and followed Zero order drug release and as n>0.89, Non-Fickian (Super case II transport). Since samples obtained from different regions have almost identical refractive indices, the Nanoemulsion may be referred to as isotropic.

Results: The optimized batch has a globule size of 122.4 nm, zeta potential of -0.26, polydispersity index of 0.187 characterized by photon correlation spectroscopy and scanning electron microscopy and 64.21% entrapment efficiency. Utilizing an artificial diffusion cell and dialysis membrane, 96.89% cumulative drug release was obtained. The assertion that the experimental and predicted values were in good agreement with a low percentage bias of less than 10% demonstrated the accuracy of the optimization process.

Conclusion: Dexibuprofen Nanoemulsion gel demonstrated prolonged drug release for up to 12 hours when compared to the micellar formulation of Ibuprofen and Dexibuprofen gel. Percent inhibition was assessed using carrageenan induced rat paw model and the anti-nociceptive effectiveness of formulations was tested using the hot plate technique. Result of ex-vivo tests showed excellent efficacy of dosage form.

Keywords: Dexibuprofen (DXI), NE (NE), Transdermal Gel, Carbopol 940, Pseudoternary phase diagram, Surface response optimization, Carrageenan, Anti-nociceptive response, Anti-inflammatory study.

Introduction:

The current study's objective is to create and develop a DXI transdermal NE gel as a twice potent formulation compared to available transdermssal formulations of Ibuprofen. DXI belongs to low soluble and highly permeable category of BCS class II. It is therapeutically active enantiomer of racemic mixture Ibuprofen which is having non-steroidal anti-inflammatory activity. After oral administration, it is only partially absorbed due to its weak solubility, and thus bioavailability varies across people. The drug's topical formulation may be limited in its efficacy due to its weak solubility in the solvent and hence low permeability. To address each of these concerns, transdermal NE could be the best solution.

Oil, water, surfactant, and co-surfactant are dispersed as transparent, monophasic, optically isotropic, and kinetically stable colloidal dispersions known as nano-emulsions with droplet sizes smaller than 500 nm.

When ultrasonic waves are used to irradiate an oil and water mixture, cavitation forces are created. This extra energy leads to the creation of nanoscale emulsion droplets at the interfaces. Without the use of surfactants, NEs may be created using ultrasonication [1]. Recent research has shown that the effectiveness of ultrasonic emulsification depends on ultrasonication strength, duration, and surfactant type [2]. The production of medicinal and food component NEs has made considerable use of ultrasonication. Compared to previous high energy methods, food grade ultrasonication NE has superior stability and smaller droplet size [3-5].

As the more concentration of surfactants responsible for skin irritation and tissue toxicity, Ultrsonication method is advantageous in this case which developes NE smaller stable and rapidly, with less utilization of surfactants and consuming less energy [6, 7].

In comparison to traditional procedures, optimization techniques offer significantly more benefits because they solve a number of challenges. These strategies demand fewer tests to establish an optimal formulation, show interactions, offer "the best" solutions in the face of competing objectives, make problem tracking and rectification more easier, and use model equations to stimulate product or process performance. Optimization approaches have recently become common place in the design and development of a wide range of dosage forms around the world [8].

Response surface approach was used to analyze formulation batches using contour plots and surface plots to find optimal excipient quantities based on its maximal responses. To attain the best potential response, a targeted value for the responses was established in the optimization plot, keeping it within the constraints of the responses already collected from the design batches. The optimization formula that may provide the desired target responses was derived from the formulation factors and levels received from the optimization plot.

Materials and methods

Materials

DXI was obtained from M/s Zuventus Healthcare Ltd., Bangalore, India, as a gift sample. Compritol 888ATO and Miglyol 812N were gifts from Glenmark Pharmaceuticals in Mumbai, Maharashtra, India. Sigma Aldrich Co. Ltd. was used to acquire carrageenan and transcutol. Oleic acid, mustard oil, castor oil, and the gelling agent Carbopol-940 were bought in Mumbai, Maharashtra, from Oxford Labchem and LOBA.

Methods:

Screening of components:

The main standard for material selection was that each component must be GRAS (Generally regarded as safe) compliant and pharmaceutically acceptable [9].

Solubility study

Screening of oil: Excess DXI was taken in a vial, 5 ml of oil was added, and the vial was then closed to determine the solubility in oils. The mixture was mixed with a vortex mixer for 30 minutes, let to sit for 24 hours, and then centrifuged for 20 minutes at 5000 rpm. After an appropriate dilution with phosphate buffer solution at 222 nm, the supernatant was collected and subjected to ultraviolet (UV) spectrophotometer analysis. Similar measurements of drug solubility in solutions containing 1% surfactants were conducted at 25± 2 °C. Experimentation was done in triplicates.

Screening of surfactant: The literature review was used to select the surfactants Tween 20, Tween 40, Tween 80, and Transcutol P for the goal of selecting the best surfactant for transdermal NE. For screening of surfactant, formulated 15% w/w solutions of the surfactants in distilled water and each solution was taken in 2.5 ml portions and placed in glass bottles. With vigorous shaking, Labrafac CC (the previously screened oil phase) was added to it drop wise until the solution became hazy.

Screening of co-surfactant: Co-surfactant was used to improve the mobility of the hydrocarbon tail of surfactant and to lower interfacial tension. Co-surfactants such as Span 20, Span 40, Labrasol, and Capryol are said to be employed in the creation of NEs and microemulsions. A pseudo-ternary phase research was conducted for the purpose of screening co-surfactant and the ratio of surfactant to co-surfactant (Smix). The aqueous titration approach was used to develop pseudo ternary phase diagrams and conducted for each mixture of oil and Smix [10-11, 16-19]. Visual observations were noted in the table after each addition of water to the oil and Smix combination. The foundation for visual observation was as follows:

- ✓ If clear and effortlessly flowable o/w NEs were produced after addition, we designated them as such.
- ✓ If the gel was clear, we referred to it as NE gel, we designated it as an emulsion if there was a milky or hazy appearance or phase separation.
- ✓ If a milky gel was produced, it was labelled as emulgel [12-13].

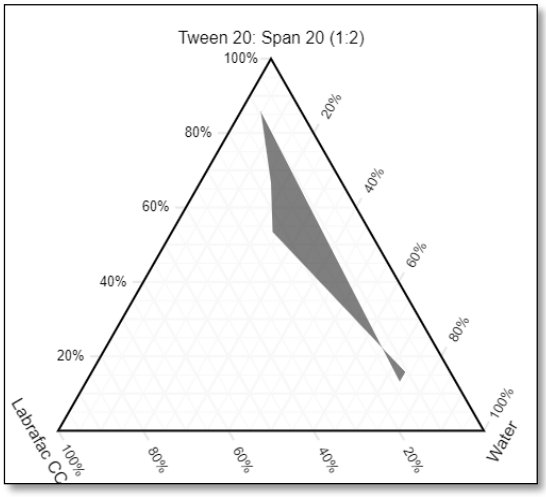

(a)

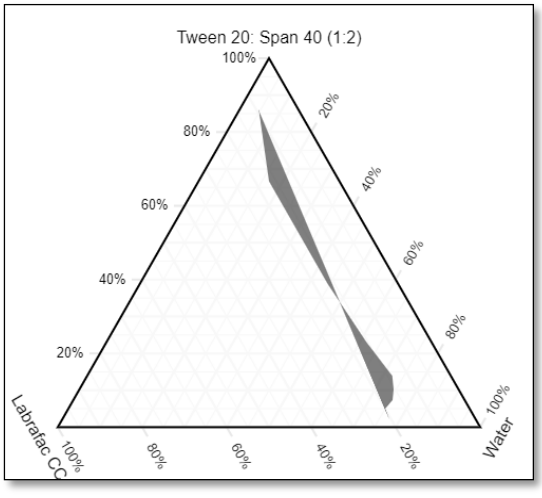

(b)

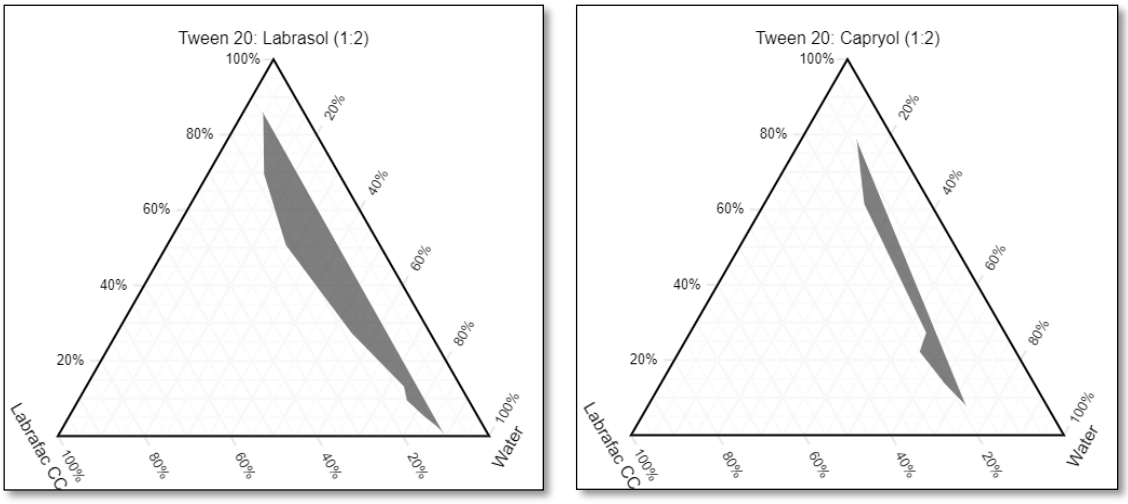

(c) **(d)**

Figure 1: Pseudo-ternary phases indicating the o/w NE region of Labrafac CC (oil), Tween 20 (surfactant) and at fix Smix ratio (1:2) with different cosurfactant indicated in Fig. a Span 20, *b* Span 40, *c* Labrasol and *d* Capryol

Effect of Smix on the formation of the NEs:

Areas where NEs occur may be quickly identified via the use of phase diagram analysis. Tween 20 and Labrasol were utilised as the surfactant and cosurfactant, respectively, in the formulation, with Labrafac CC as the oil phase. For the ternary phase experiment, different volumes of oil (1:9, 1:8, 1:7, 1:6, 1:5, 1:4, 1:3, 1:2, and 1:1) were mixed with various ratios of surfactant and cosurfactant (1:0, 1:1, 1:2, 1:3, and 1:4). Pseudo ternary phase diagrams were produced using the aqueous titration method. There was a separate slow titration with aqueous phase for each mixture of oil and Smix [14].

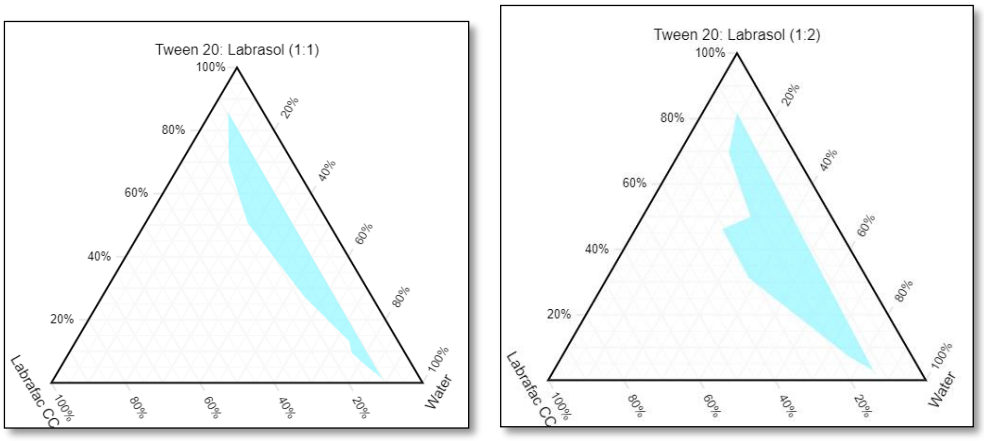

(a) **(b)**

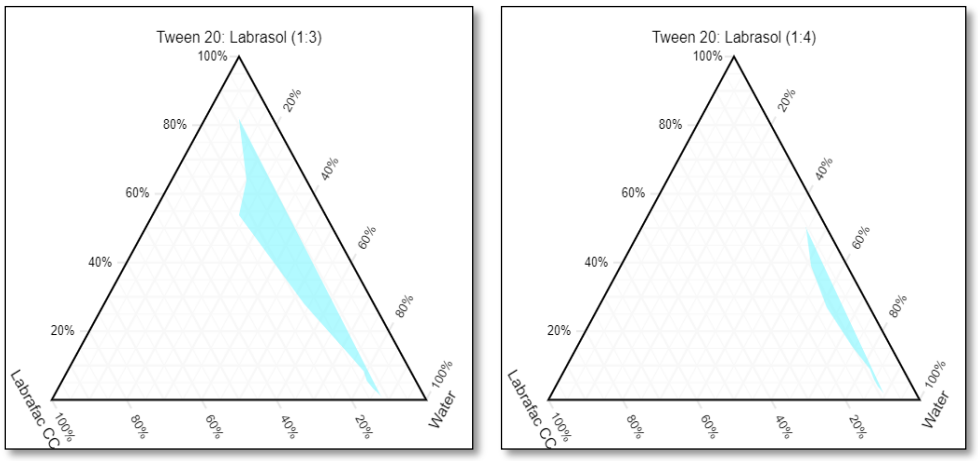

(c) **(d)**

Figure 2: Pseudo-ternary phase diagrams of o/w NE region of Labrafac CC(oil), Tween 20 (surfactant) and Labrasol (cosurfactant) at different Smix ratios indicated in Fig. a (Smix 1:1),*b* (Smix 1:2), c (Smix1:3) and d (Smix1:4)

Method of Preparation of NE:

Aqueous phase titration or spontaneous emulsification method used to prepare NE. The size reduction was accomplished using a probe sonicator from Sonics and Material Inc. USA, which has a 6 mm-diameter probe and operates at a 20 KHz frequency. To limit heat generation by the probe sonication, an apparatus was built up to perform the emulsification and sonication spontaneously at a regulated temperature by supplying a cold environment of an ice bath. According to the procedure, a measuring cylinder was used to collect the first measured quantity of oil and Smix. The water phase was then added using a burette, and sometimes the mixture was sonicated. The whole set-up was submerged in an icy water bath [20].

Preparation of Nano-Emulsion gel:

The Carbopol 940 was dissolved in a sufficient amount of water to produce the gel. Carbopol 940 solution was left in the dark for 24 hours after full dispersion. The NE then incorporated in gel. Triethanolamine was then added to neutralise the gel.

Design of Emulsion physical stability:

The stability of the emulsion to centrifugation was investigated by centrifuging it at 10,000 rpm for 30 minutes after ultrasonic emulsification. In order to study intrinsic stability, the emulsion was kept at room temperature. Then any phase separation or creaming was looked for. Additionally, variations in droplet diameter were investigated throughout time.

Design of experiment and optimization of NEs:

Oil (X1) and Smix (X2) were the two main formulation-affecting variables, and globule size (Y1), % entrapment efficiency (Y2), and % drug release (Y3) were the three main responses that needed to analysis. The experimental design utilised was a three-level two-factorial design. Based on the optimal oil concentrations, Smix (Surfactant: Co-Surfactant) established from the pseudo-ternary phase diagram, formulation batches are created [21-24].

Table 1:3^2 full factorial design containing dependent and independent variables

Independent variables	Dependent variables
X_1 = Oil X_2 = Smix	Y_1 = Globule size Y_2 = Entrapment efficiency Y3 = Drug release

Table 2: Formulation composition as per factorial design

Code	Level 1	Level 2	Oil (ml)	Smix (ml)	Water (ml)	Percentage of Oil	Percentage of Smix	Percentage of Water
F1	-1	-1	3	8	9	15	40	45
F2	-1	0	3	9	8	15	45	40
F3	-1	+1	3	10	7	15	50	35
F4	0	-1	3.5	8	8.5	18	40	43
F5	0	0	3.5	9	7.5	18	45	38
F6	0	+1	3.5	10	6.5	18	50	33
F7	+1	-1	4	8	8	20	40	40
F8	+1	0	4	9	7	20	45	35
F9	+1	+1	4	10	6	20	50	30

Result of optimization:

To determine precisely where the NE falls, no drag was used in the construction of any phase diagrams. Since it is well recognised that excessive surfactant usage may irritate the skin [26-28], it is crucial to accurately calculate the surfactant concentration and apply the right quantity of surfactant in the formulation. The formulations for the research were chosen from pseudo-ternary phase diagrams where the amount of oil phase fully dissolves the medicine and where the amount of Smix and distilled water is optimal [29].

Preparation of DXI loaded NE gels:

The ideal formulation of DXI-loaded NE with 5% DXI was employed in gel bases. Carbopol 940 was used at 1% concentrations as a gelling agent in the production of gel bases. The measured quantity of carbopol was diluted in deionized water and given a whole night's

worth of darkness to hydrate. The dispersion was neutralised with triethanolamine and stirred for a further two to three hours. The gel base was then supplemented with the DXI-loaded vesicular carriers and mixed for an additional hour before being kept at 4°C for further investigation [39-40].

Characterization:

Characterization of NE:

Physical stability studies for DXI NEs:

At a certain concentration of oil, surfactant, and water, NEs are physically and thermodynamically stable systems that form without phase separation, creaming, or cracking. Nano- or microemulsions are distinguished from emulsions that have kinetic stability and will ultimately phase separate by their thermostability [30]. Therefore, several physical stability experiments, including centrifugation, heating and cooling cycles, freeze-thaw cycles, and long-term stability tests, were performed on the chosen formulations. The formulations that passed physical stability testing were kept for further research.

Stability studies of prepared NEs:

Centrifugation, freezing and thawing cycles, as well as heating-cooling cycles, were used to conduct stability experiments on the produced NEs [34-35].

i. Heating-cooling cycle: Six cycles were carried out between 4 and 45 degrees Celsius with storage at each temperature lasting 48 hours, and the stability of the created NEs was assessed (transparent with no phase separation).
ii. Test of centrifugation: The prepared NEs were centrifuged for 30 minutes at 3,500 rpm while being checked for transparency and the lack of phase separation.
iii. Freeze-thaw cycle: Three freeze-thaw cycles of the NEs between -21°C and +25°C for 48 h were performed and observed for transparency and absence of phase separation.

Percentage Transmission:

The homogeneous formulations were tested against water for transmittance at 630 nm and analysed for percent transmittance using a UV-Vis spectrophotometer (UV-1800, Shimadzu, Japan).

Refractive Index and pH:

Using an Abbe's type refractometer, the formulations were further assessed for determining the refractive index (Guru Nanak Instruments, Delhi, India). At a temperature of 25°C ± 1°C, a pH meter (Equip-Tronics, model no. EQ-610) and a conductivity metre (Equip-Tronics, model no. EQ-660A) were used to measure pH and conductivity.

Filter paper test and Dye test:

An o/w NE will expand out quickly when placed onto filter paper, which is the basis for the filter paper test. A w/o NE, in the opposite hand, will only spread slowly [36]. On the other hand, each NE composition also contained a water-soluble pigment (methyl orange). If there was no precipitation and the pigment blended evenly with the NE, the NE pattern is o/w [37].

Entrapment Efficiency:

To take apart the oil and aqueous phases, 2 ml of drug-loaded material spun at 10000 rpm for 30 minutes at 20°C in a chilled centrifuge. After the sample was diluted with methanol and filtered using 40m filter paper, its absorbance was measured at 222 nm with a UV-VIS spectrophotometer. The entrapment efficiency estimated using the following equation,

$$\text{DEE \%} = \frac{\text{Total amount of drug added} - \text{Amount of drug in aqueous layer}}{\text{Total amount of drug added}} \; X\,100$$

Drug Content:

For the evaluation of drug content, 1 g of NE was mixed with 99 mL of phosphate buffer solution at pH 7.4 for 24 h with continuous stirring on a magnetic stirrer. The clear solution obtained was analyzed at λ max 222 nm via UV spectrophotometer

Optical measurement:

Visual inspection was done of the physical state of the finished samples after high pressure homogenization. A successful formulation of a NE was defined as a transparent solution free of crystals.

Globule size & surface morphology:

To determine the homogeneity of globules, the breadth and range of droplet size, and the distribution of surface charges, one uses a particle size measuring method, such as the Poly-dispersity index (PDI) or Zeta potential (ZP). The more zeta potential and the lower the PDI value (0.2), the more stable NE is against other destabilizing influences.

Photon correlation spectroscopy (PCS) and dynamic light scattering (DLS) are tools used to measure particle size.

Size distribution and droplet size are calculated from group observations of sample dispersion via DLS, i.e. NE. The Zetasizer is used to measure ZP, which is the potential charge difference between the particles and continuous phase [38].

Viscosity determination:

Using a Brookfield viscometer, the viscosities of the formulations were assessed. A 25 ml beaker containing 20 ml of NE was filled, and spindle number 6 was used to test the viscosity at a speed of 10 rpm.

In vitro drug release study:

Franz diffusion cell and cellophane membrane are used to conduct the diffusion investigations of the produced NEs. A NE sample (5 ml) is taken in a cellophane membrane, and diffusion tests are conducted at 37 °C with a dissolving medium of 250 ml of (25%) methanolic-phosphate buffer (pH 7.4). To maintain the sink condition, 5 ml of each sample were regularly removed at intervals of 1, 2, 3, 4, 5, 6, 7 and 8 hours, and each sample was replaced with an equal amount of new dissolving media. Samples are examined for drug content using a UV spectrophotometer at 222 nm.

Kinetic Modelling of Drug Release:

The sequence and mechanism of drug release from all vesicular suspensions were discovered by fitting the In vitro drug release data into the subsequent mathematical models. The drug release kinetics from all formulations were examined using the linear regression method.

Statistical Analysis:

The degree of significance of the examined factors on the globule size, EE, and drug release of the produced formulations was assessed using an ANOVA analysis. As P-values less than 0.0500 indicate that model terms are significant, the ANOVA results indicated that the oil and Smix concentration had a significant influence on all variables. Model terms are not significant if the value is higher than 0.1000.

Response Surface Plot:

We were able to construct a response surface counter plot using the quadratic model discovered by regression analysis, in which the dependent variable Y was represented by a curvature surface as a function of Xi. The response surface plot immediately illustrates the link between the response and independent factors.

Optimization of NE:

Utilizing controlled drug release across the diffusion membrane, minimizing of globule size, maximizing of encapsulation efficiency, and other optimization goals, the best formulation setting was created utilising a constrained optimization approach. The programme forecast optimal formulations, which were then contrasted with the findings of the experiments [39-41].

Characterization of NE Gel Based on Gel Characteristics:

The pH, spreadability, gel strength, extrudability, and drug release and permeation tests of the drug-loaded NE integrated gels as well as micellar gels (without carrier system) were assessed using techniques from the literature, as indicated in Table 8.27 [42-48].

Determination of pH:

The pH of the gels was measured at room temperature using a digital pH metre. The pH metre was first calibrated with standard buffers of pH 7, after which 10 g of gel was weighed and dissolved in 25 ml of distilled water. The pH was then determined by dipping the electrode of the pH metre into the dissolved gel.

Spreadability:

A pre-marked glass slide was covered with a second glass slide after a 0.5 g gel sample was put in a circle on the first glass slide with a diameter of 1 cm. A weight of 2 g was let to rest on the top glass slide for one minute. The gel's dispersion led to an increase in diameter. In order to determine spreadability, the following formula was used:

$$S = M.L / T$$

Where S stands for spreadability, M for the weight fastened to the higher slide, L for spread, and T for time.

Gel strength:

The tool for measuring gel strength consisted of a plunger with the other end submerged in the gel and a pan on one end to store weights. A glass container containing the prepared gels was marked 1 cm below the filling mark.

The weight required for the plunger to penetrate the created gel at a depth of 1 cm was calculated for each formulation.

Extrudability:

The gel was prepared, poured into a tube, and sealed. Near the bottom of the tube, 3 marks were made, spaced 1.5 cm apart. On a Pfizer hardness tester, the tube was pressed at the marking with a pressure of 1 kg/cm2, and for each formulation, the weight of gel released in the form of a continuous ribbon as well as the uniformity of gel release from the tube were measured.

Rheological studies:

The gels' viscosity was measured using a Brookfield viscometer. The viscometer's spindle number 6 was affixed after the gel had been placed within the sample container. The spindle was dropped perpendicularly into the sample and then allowed to revolve at a constant, ideal speed at room temperature in order to produce a torque of at least 10%. Different rpms were used to test the formulation's viscosity measurements.

Release studies of drug carriers based transdermal gel:

In-vitro drug release studies were carried out using a modified Franz diffusion cell and a dialysis membrane. Dialysis membrane was used to seal one side of a two-sided, open-ended glass tube (HiMedia Laboratories Pvt. Ltd., M.Weight cut off: 12000). A 250 ml Beaker was used as the receptor compartment, and 100 ml of phosphate buffer saline was added to the donor compartment, which was the built tube into which 1 gm of gel was inserted. 12 hours of dialysis were performed at 37±0.5°C. Every hour, 2ml of pH7.4 PBS

from the receptor compartment was drained and replenished with an equal amount of fresh diffusion fluid to maintain sink conditions. A UV spectrophotometer was used to analyze the isolated receptor fluids at 222 nm after being properly diluted. Table 8.28 and Figure 8.39 both visually depict the in vitro drug release from NE gels.

Comparative study of micellar and NE gel:

According to the technique protocol stated under "Materials and Methods" and DXI loaded NE gel and micellar DXI gel were made.

Ex-vivo skin permeation studies:

Goat skin was used for the study. Carefully dissected subcutaneous (SC) tissues and adhering fats were removed from the goat skin by rubbing it with cotton. The excised full thickness skin samples were adjusted before to the experiment by soaking for around an hour in a PBS solution with a pH of 7.4 and a temperature range of 4–8°C. The vertical Franz diffusion cell's donor and receptor chambers were then firmly positioned between the skin samples. The dermis was put in the receptor compartment (50 mL of PBS pH 7.4) at 32°C, while SC was put in the donor compartment. 1mL of one of the formulations was charged into the donor compartment. At predetermined intervals (0.5, 1, 2, 4, 6, 8 and 24 h), samples of the receptor fluid (3 mL) were obtained and the cell was replaced with an equal amount of newly generated receptor fluid. Plotting against time was the cumulative quantity of medication that pierced the skin per unit area (mg/cm2) (h). According to the following equations [49-53], the flow (Jmax) at 24 hours was calculated:

$$Jmax = \frac{\text{Amount of drug permeated}}{Time\ X\ area\ of\ membrane}$$

Anti-inflammatory activity:

Carrageenan-induced rat paw oedema: Digital caliber was used to assess the DXI NE gel's anti-inflammatory effects. Male Wistar rats weighing between 180 and 200 grams were used in the experiment. Four groups of five rats each were formed out of the rats. Group I was a control while formulation was applied to Groups II, III, and IV, respectively, at the site of inflammation using Test1- Micellar IBU gel, Test2- Micellar DXI gel, and Test3- DXI NE gel. The anti-inflammatory qualities of the formulation were assessed using the paw edoema approach, which is based on the suppression of the volume of hind edoema caused by a phlogistic medication. In this investigation, a phlogistic agent consisting of 1% w/v carrageenan solution in 0.9% saline solution was used.

$$Oedema\ Rate\ (E) = \frac{V_t - V_0}{V_0}$$

$$Inhibition\ Rate\ (I) = \frac{E_c - E_t}{E_c}$$

Where Vo stands for the average paw volume before the carrageenan injection and Vt for the average paw volume after the injection. Ec stands for the edoema rate in the control group whereas Et stands for the oedema rate in the treatment group. Following delivery of -carrageenan, the initial volume of the paws as well as the volume of inflamed paws were measured at 1, 2, 4, 6, 12, and 24 hours. A graph showing percent inhibition against time was created [54].

Anti-nociceptive activity:

Hot plate test: Twenty male mice were divided into four groups, each with five mice: Group I, the untreated control group; Group II, the micellar IBU gel therapy; Group III, the micellar DXI gel treatment; and Group IV, the DXI-loaded NE gel treatment. All mice had two training sessions on the hot plate for a minute: one 20 minutes prior to the baseline nociceptive threshold measurement and the other 24 hours prior to the test. On a

heated plate that was kept at a constant temperature of 55 °C, then the animal was put on the hot plate, and the nociceptive response was measured from that point on until the animal displayed any response, such as licking its feet, attempting to jump away, or lifting its limbs. Hot-plate latencies were assessed at various points (0.5, 1, 2, 3, 4, and 6 hours) after the formulations were applied after the baseline nociceptive threshold had been established. The cut-off time was set to 30 seconds in order to prevent damage to animal tissue [55-57].

Stability Studies:

The stability of optimal DXI loaded NE was tested in accordance with ICH guidelines as follows:

Condition:

1. Accelerated stability study: 25°C ± 2°C/60% RH ± 5% RH

2. Long term stability study: 4-8°C ± 1°C

Particle size, zeta potential, transdermal flux, and encapsulation effectiveness of the improved formulation were examined during storage. Drug NEs were kept in screw-capped glass vials and kept in the refrigerator and at 25°C, 2°C, and 60%, 5% RH for three and six months, respectively (Singh et al., 2011). One gram of each sample was used to visually assess the dispersions' physical stability every three and six months [58-59].

Result:

Screening of components:

According to the investigation, Tween 20 has a strong solubilization ability for Labrafac CC oil. Tween 20 was used as the surfactant to create DXI NE.

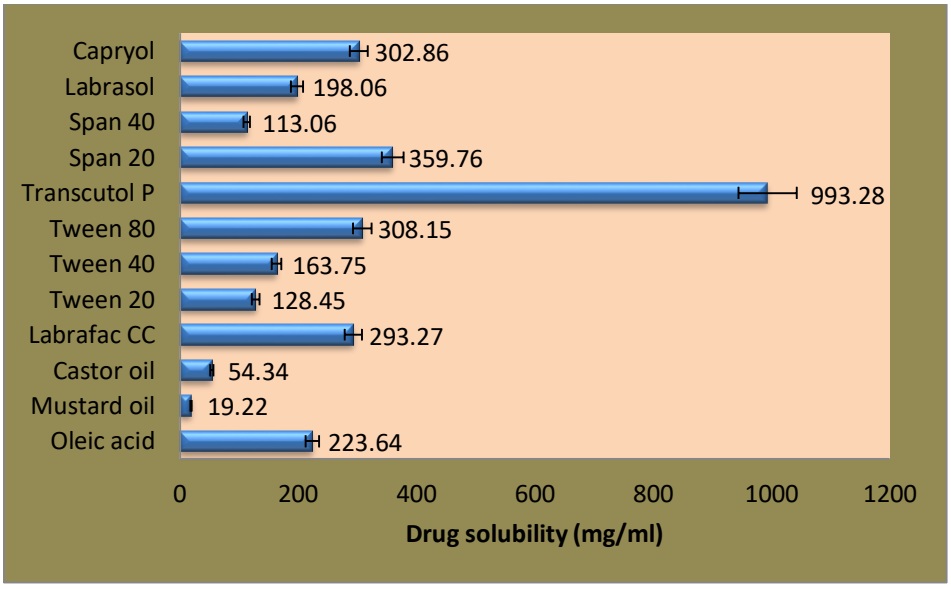

Figure 3: Solubility of DXI in different component

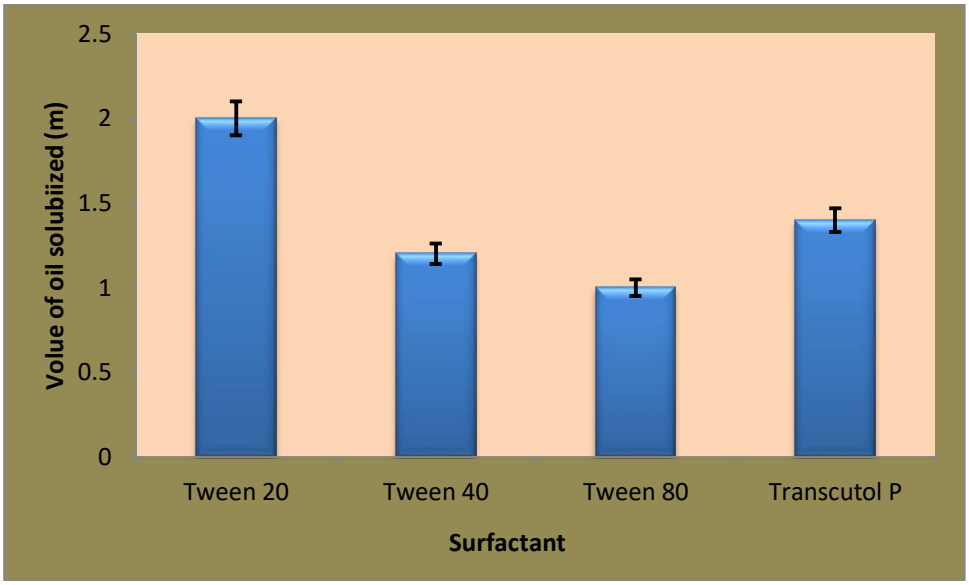

Figure 4: Surfactant and its capacity to solubilize Labrafac CC oil in ml

Span 20, Span 40, Labrasol, and Capryol were used to produce various pseudo-ternary phase diagrams. The analysis made it evident that Labrasol had created a larger area of NEs than Span 20, Span 40, and Capryol.

Labrasol was chosen as the cosurfactant as a result.

According to Figure, the maximum area of NEs was shown by the Smix ratio of 1:2, followed by 1:1. The creation of a NE with poor flow properties was caused by the Smix ratio of 1:1, which demonstrated poor flow properties.

Refractive Index:

Table 3 contains a list of the parameters for NE characterization. The NEs may be referred to as isotropic since the refractive indices of samples taken from three different regions of the sample are almost equal, as shown by minimum standard deviations.

Globule size, zeta potential analysis:

The average droplet size for each sample was significantly below 200 nm and well within the nanometric range. Low polydispersity index values in every NE sample pointed to an uniform droplet size distribution. For droplet stability, the zeta potential values fell within allowable bounds. Since the gel stiffness provides stability to the droplet gels against likely coalescence, the zeta potential values are less significant in the case of gels (Table 3).

Table 3: Refractive Index, Globule size, zeta potential and Polydispersity Index of NE formulations

Formulation	Refractive Index	DEE (%w/w)	Globule size (nm)	Zeta Potential	Polydispersity Index	% Drug release
F1	1.381±0.013	42.14±1.2	143.5±2.3	-28.34±0.72	0.143±0.052	88.61 ±2.94
F2	1.387±0.021	42.63±1.0	129.2±3.6	-30.46±0.89	0.298±0.046	91.78 ±2.86
F3	1.410±0.007	55.46±0.7	106.3±3.1	-26.51±1.32	0.153±0.016	99.08 ±3.06
F4	1.396±0.012	48.78±1.5	156.1±2.5	-22.89±0.56	0.106±0.010	86.69 ±2.66
F5	1.428±0.061	62.43±1.3	136.7±3.4	-26.66±1.16	0.198±0.036	91.12 ±2.56
F6	1.394±0.022	64.59±1.1	119.2±3.8	-29.54±1.24	0.164±0.020	97.32 ±2.66
F7	1.406±0.008	48.98±1.4	172.3±2.9	-28.74±0.69	0.176±0.008	87.04 ±2.72
F8	1.393±0.010	59.30±1.3	148.5±2.1	-32.62±1.34	0.154±0.013	89.2 ±3.11
F9	1.406±0.032	62.12±0.7	128.4±1.4	-30.96±0.76	0.283±0.061	92.12 ±2.74

* S.D. (standard deviation calculated after triplicate observation n=3)

The zeta potential for each formulation is shown in Table 3. An essential instrument for forecasting NE stability is the zeta potential. Zeta potential values of less than -25 mg are regarded as suitable for NEs stability [59]. The range of the zeta potential was -22.890.56 mV to -32.621.34 mV. As a consequence, it is anticipated that the majority of formed NEs will remain stable.

Drug entrapment efficiency:

The DXI NE batch F6 indicated the highest drug entrapment efficiency 64.59%, whereas the most of the batches showed entrapment efficiency more than 50%. Oil (Labrafac CC) clearly had a key role in improving DXI entrapment efficiency. The drug entrapment efficiency of the formulation with lower oil (3ml) was poorer than that of the formulation with higher oil (4ml) content (Table 3).

As indicated in Figure, the entrapment efficiency of NE increased with increasing oil and decreased with increasing Smix concentration.

In vitro drug release:

For in vitro drug release testing, artificial diffusion cells were used for all formulations. It was shown that the percentage medication release reduced when oil concentration increased, but the percentage drug release increased as Smix concentration increased (Table 4).

Table 4: Cumulative drug release from DXI NE formulations

Time (Hrs) / Batches	1	2	3	4	5	6	7	8	9	10	11	12
F1	4.45 ±1.26	19.24 ±1.12	32.23 ±1.56	44.87 ±2.04	58.12 ±2.54	63.9 ±2.17	70.12 ±2.61	79.04 ±2.73	84.15 ±3.41	86.12 ±2.58	86.89 ±3.74	88.61 ±2.94
F2	5.12 ±1.13	19.65 ±2.10	38.08 ±1.36	48.86 ±2.14	61.23 ±2.51	69.46 ±2.62	75.94 ±2.68	76.27 ±2.87	80.74 ±3.54	86.56 ±3.20	89.12 ±3.04	91.78 ±2.86
F3	7.26 ±0.96	24.62 ±1.65	38.12 ±2.14	51.22 ±1.89	64.09 ±1.94	71.23 ±2.66	79.32 ±2.45	86.66 ±2.47	90.75 ±2.10	95.94 ±3.02	97.26 ±3.10	99.08 ±3.06
F4	3.94 ±1.03	17.13 ±1.52	26.86 ±1.68	36.54 ±1.86	44.76 ±2.54	58.5 ±2.56	64.67 ±3.14	71.10 ±2.47	79.38 ±2.32	82.24 ±3.14	85.12 ±3.06	86.69 ±2.66
F5	4.82 ±0.95	18.65 ±1.56	28.09 ±2.14	39.14 ±2.32	46.16 ±2.46	61.81 ±1.98	67.92 ±2.62	73.52 ±2.10	83.21 ±1.69	86.54 ±2.64	89.62 ±2.74	91.12 ±2.56
F6	5.12 ±1.02	21.54 ±1.22	32.14 ±2.62	48.89 ±1.12	52.22 ±2.23	64.73 ±1.49	70.85 ±1.98	79.06 ±2.62	86.73 ±3.10	92.87 ±3.22	95.12 ±2.92	97.32 ±2.66
F7	5.22 ±1.12	16.78 ±1.52	21.65 ±1.64	38.54 ±2.24	46.56 ±2.58	52.24 ±1.86	68.66 ±2.46	76.32 ±2.44	82.74 ±3.10	84.13 ±2.92	86.21 ±3.25	87.04 ±2.72
F8	5.31 ±1.04	16.87 ±2.42	29.61 ±2.74	35.72 ±3.04	41.06 ±3.84	54.68 ±3.12	61.12 ±2.86	69.03 ±3.23	76.89 ±2.56	81.26 ±2.68	87.34 ±2.95	89.2 ±3.11
F9	5.22 ±0.89	21.65 ± 1.06	33.46 ±2.12	47.16 ±2.16	58.24 ± 2.63	67.89 ±2.08	70.12 ±2.54	80.85 ±2.35	86.47 ±2.66	90.45 ±1.98	91.63 ±2.37	92.12 ±2.74

Table 5: Summary of Release kinetics data of all DXI NE formulations

Time (Hrs) / Batches	Zero order	First order	Higuchi	Hixson crowel	Korsmeyer rpeppas	n	Mechanism of drug release
		R2	R2	R2	R2		
F1	0.9878	0.9762	0.8755	0.9838	0.9763	1.11	Zero Model Non-Fickian (Super case II transport)
F2	0.9866	0.9773	0.8801	0.9855	0.9803	1.30	Zero order Non-Fickian (Super case II transport)
F3	0.991	0.9812	0.9016	0.9903	0.9822	1.19	Zero order Non-Fickian (Super case II transport)
F4	0.9908	0.9633	0.8671	0.9766	0.961	1.32	Zero order Non-Fickian (Super case II transport)
F5	0.99	0.9558	0.871	0.9722	0.9578	1.25	Zero order Non-Fickian (Super case II transport)
F6	0.9832	0.974	0.8879	0.9815	0.9782	1.24	Non-Fickian (Super case II
F7	0.9822	0.972	0.8682	0.977	0.9519	1.26	Zero order Non-Fickian (Super case II transport)
F8	0.986	0.9717	0.8909	0.9799	0.9681	1.06	Zero order Non-Fickian (Super case II transport)
F9	0.9925	0.9763	0.8846	0.9869	0.9778	1.89	Zero order Non-Fickian (Super case II transport)

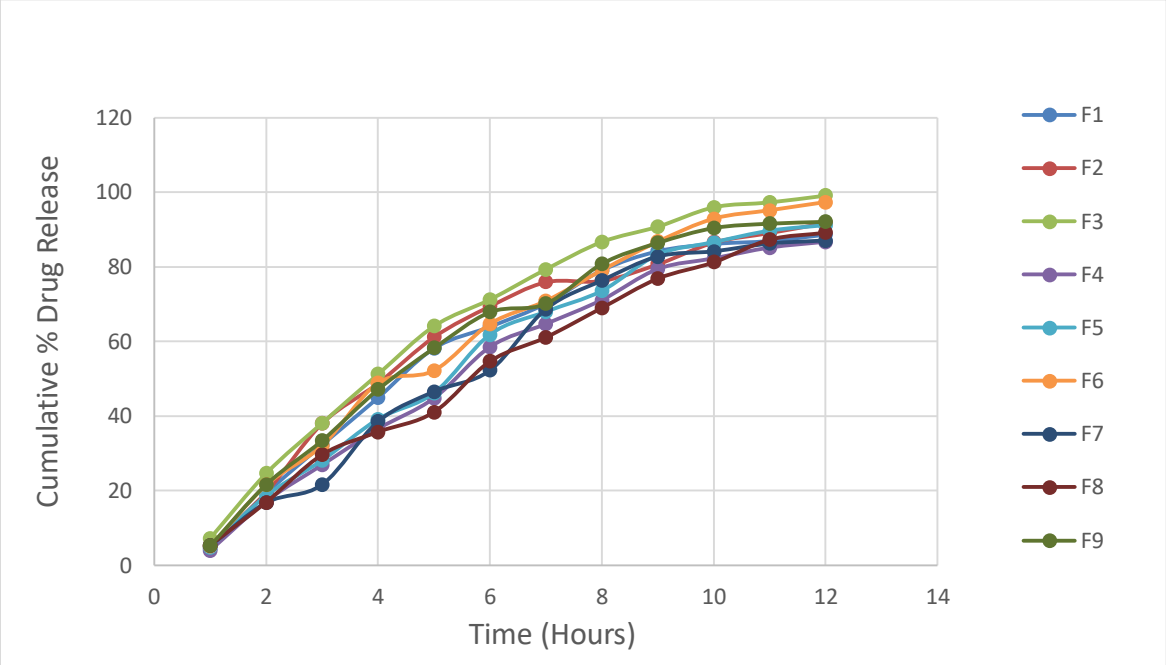

Figure 6: Cumulative % Drug Release profiles of DXI NE batches

Release Kinetics studies:

R2 and n values were calculated from linear curves and then used to feed the curve fitting findings into a variety of release kinetics mathematical models. The data analysis utilised the value of the resulting regression coefficients. All formulations generally adhered to Zero order release kinetics with good regression coefficients (R2) (Table 5). A value of n (Release exponent) larger than 0.89 indicated that the drug is released from the body through the Super Case II transport mechanism, which is specified by the model Korsmeyer-Peppas equation.

Central composite optimization results:

Response surface plot:

The relationships between NE composition factors (such as oil and smix) and responses (such as Globule size, entrapment efficiency and drug release) may be better understood by examining a number of contour plots. Figures 3a and 3b indicate that when the overall oil content rose, the size of the NE globules also grew. Surfactant concentration had an impact on globule size. Figures show that when the Smix concentration rose, NE globule size shrank. This may be because surface tension decreased as surfactant concentration rose.

Utilizing three-dimensional response surface graphs, the interplay of the components was shown. The model showed that on their own, the two examined factors had a significant influence on globule size (Figure 3 a & b). The 3-D figure shows that the globule size rose from 106.3±3.1 nm to 172.3±2.9 nm in the NE at greater & lower levels of oil, respectively, and reduced from 143.5±2.3 nm to 106.3±3.1 nm in the NE at lower & higher levels of surfactant, respectively.

Entrapment efficiency of NE enhanced with increasing oil and reduced with increasing Smix concentration as shown in Figure 4 a & b.

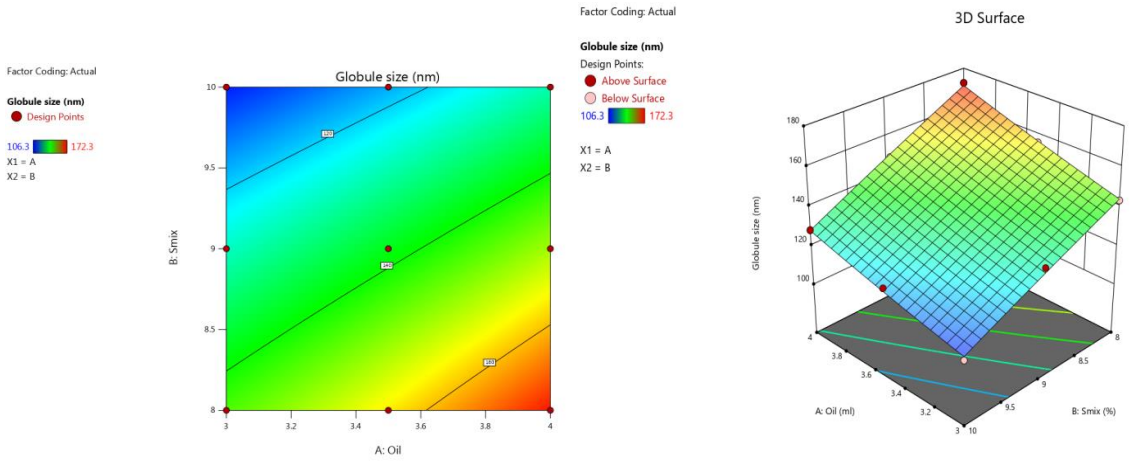

Figure 3 a & b. Effects of interaction of oil and Smix on NE globule size

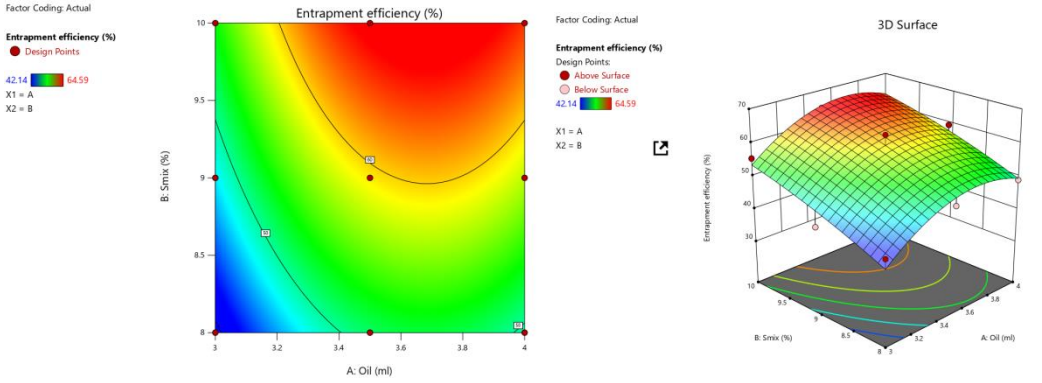

Figure 4 a & b. Effects of interaction of oil and Smix on DXI entrapment efficiency

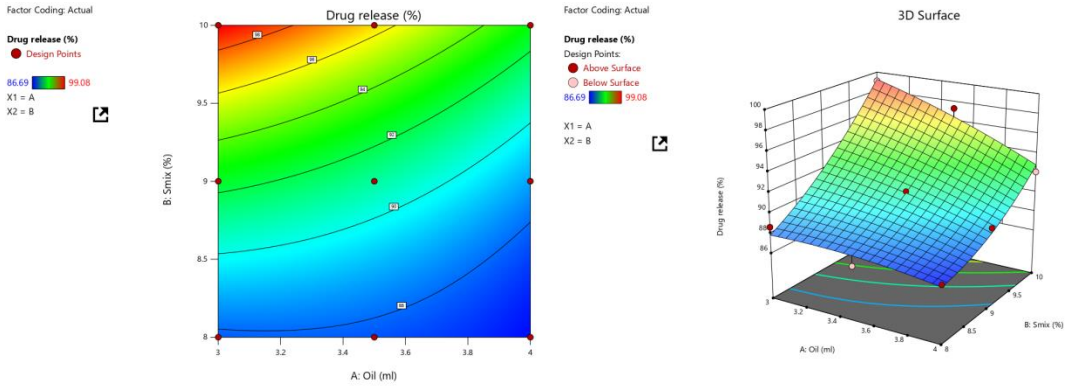

Figure 5 a & b. Effects of interaction of oil and Smix on NE drug release

Figure 5 a shows that a drop in oil concentration and a rise in Smix concentration led to an increase in NE drug release.

To display the interaction of the factors, the three-dimensional response surface graphs were produced. Both of the criteria under investigation had a considerable independent impact on the drug release, the model showed. According to the 3-D counter plot, the drug release dropped at higher concentrations of oil and Smix, going from 66.4 % to 56.56 %.

ANOVA Study:

According to the ANOVA findings the Oil and Smix concentrations had a significant influence on all variables. Low P values

(<0.05) indicated that the particular model was significant. The predictors are not significant if the P-value is greater than 0.1. Model F-values for globule size, Entrapment efficiency and percent drug release of a NE was 98.84, 18.34 and 46.85 respectively, which indicates that it is a significant model. Noise may be the root cause of a high F-value.

Final Equation in Terms of Actual Factors for globule size:

$+121.04167+33.95X1+1.05833X2-3.35X_1X_2+2.8X_1^2-0.5X_2^2$

Equation for percent entrapment efficiency:

$-385.37+212.56X_1+19.72X_2+0.41X_1X_2 - 29.31X_1^2-1.60X_2^2$

Equation for percent drug release:

$+105.45-5.92X_1-2.52X_2$

In this regression equation, positive numbers before a factor indicate that the answer grows as the factor rises and vice versa. It has been shown that the globule size of the NEs increases when the Oil and Smix rises. This impact may be explained by the fact that an increase in NE.

Characterization of Optimized batch of NE:

Desirable (Constrained) Optimization of NE:

Constrained optimizations aid in the discovery of the best NE formula that satisfies our requirements for the smallest homogeneous and stable globule size, the highest entrapment efficiency, and 12-hour release. The final modified experimental settings were created and evaluated to provide a combination of factor values by reaching a compromise among a range of possible responses. The optimized formula was created and its results were studied in order to verify the predicted optimum factor values and their anticipated responses.

An optimization strategy that was limited was used to get the optimized NE. Software suggested formulations showed accurate actual and anticipated values (low error percentage), demonstrating the validity of the optimization approach. Particle size, zeta potential, polydispersity index, drug release, and entrapment effectiveness were all assessed for the improved formulation. Tables 6 provide the optimization results from desirable optimization.

Table 6: Composition of the Optimized Formulation of DXI NE Obtained by Constrained Optimization Technique and Comparison of Experimental and Predicted Values

Optimized formulation of DXI NE					
Ingredients				**Optimized amount**	
Oil				3.610	
Smix				8.243	
Evaluated for	Globule size (nm)	Zeta potential (mV)	PDI	% Entrapment efficiency	% Drug release after 12 hrs.
Predicted	128.897	-	-	62.085	92.1894
Experimental	122.4	-0.26	0.187	64.21±2.06	96.13 ±1.92

Globule size and morphology:

The morphology of oil globules may be seen with a very high level of detail using Transmission electron microscopy (TEM). Figure illustrates the results of the improved formulation's scanning. Oil globules seemed round and round in the picture that was acquired.

As shown in Figure, the experimental globule size of the optimized NE (122.4 nm) was found to be quite similar to the expected globule size (128.897 nm). A low percentage bias of 5.04% (<10%) observed based on the difference between the experimental value and the predicted value, proving the accuracy and reliability of optimization process.

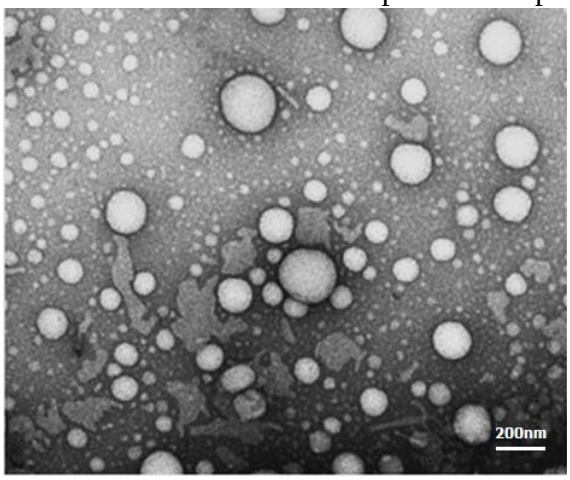

Figure 6: TEM of DXI NE

		Size (d.nm):	% Intensity:	St Dev (d.n...
Z-Average (d.nm): 122.4	Peak 1:	154.1	97.0	66.38
PdI: 0.187	Peak 2:	33.95	3.0	6.305
Intercept: 0.932	Peak 3:	0.000	0.0	0.000
Result quality : Good				

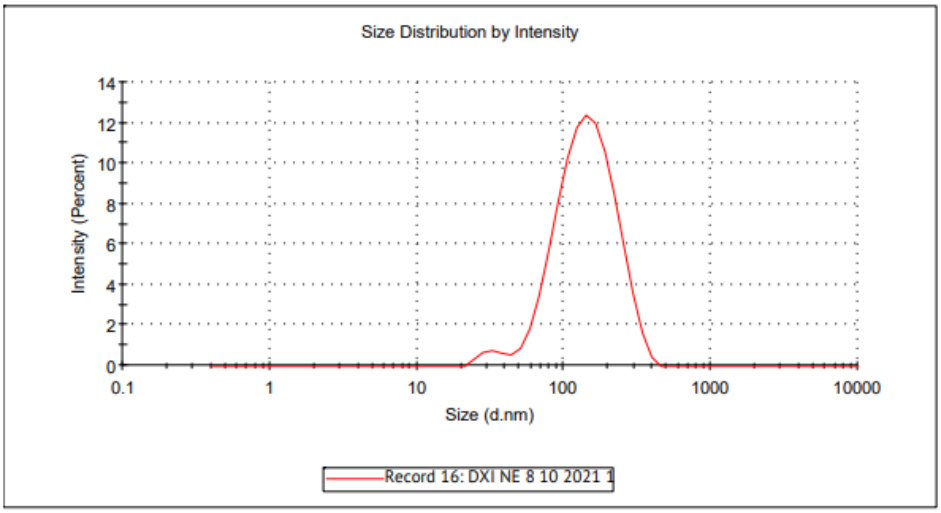

Figure 7: Size distribution of optimized DXI NE

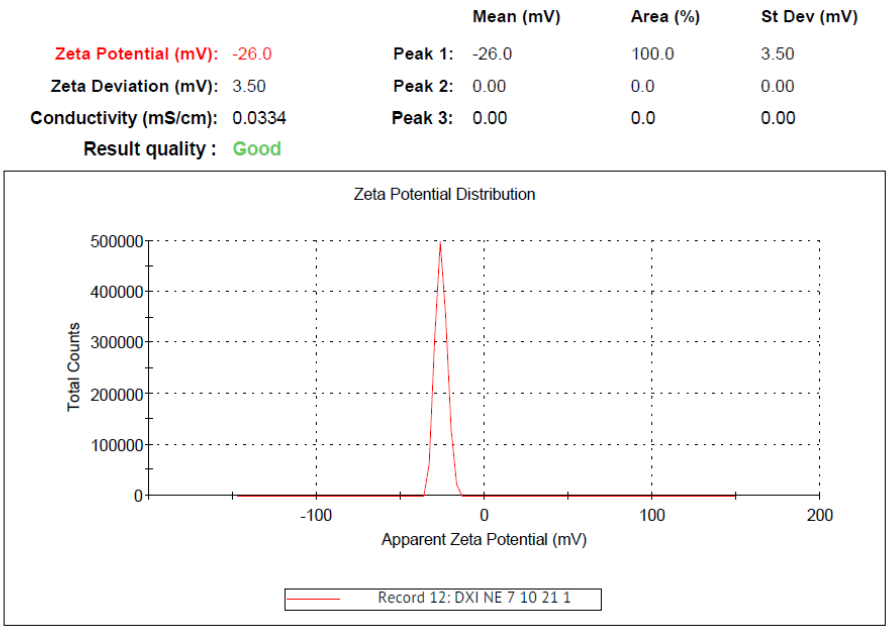

Figure 8: Zeta potential of optimized DXI NE

Zeta Potential and PDI:

Zeta potential of the DXI NE optimized formulation was found to be -26.0, indicating the stability of the NLC formulation. Zeta potential values of less than -25 mV and more than +25 mV are regarded as adequate for NE stability. Polydispersity Index values between 0.2 and 0.3 indicate globule homogeneity. As shown by the PDI observed 0.187, the optimized batch of DXI NE has relatively homogeneous globules.

Entrapment efficiency:

With a low percentage bias of 3.42%, the experimental and projected entrapment efficiency values in the fresh batch of NE were determined to be 62.085% and 64.21%, respectively. Based on low percentage bias values of < 10%, it was claimed that the experimental and anticipated outcomes of formulations were in excellent agreement, demonstrating the validity of the optimization process.

Drug release:

The anticipated and experimental values of drug release in the optimized batch were found to be 92.1894% and 96.13%, respectively, with a low percentage bias less than 10%. The correctness of the optimization method was shown by the statement that the experimental and anticipated values of the modified formulation were in excellent agreement.

Table 7: Release kinetics data of optimized DXI NE

Batch	**Zero order**	**First order**	**Higuchi Model**	**Hixson crowel Model**	**Korsmeyer-peppas Model**	**n**	**Mechanism of drug release**
	R^2	**R^2**	**R^2**	**R^2**	**R^2**		
R2	0.9898	0.9812	0.0.9145	0.9816	0.9899	1.16	Zero order Non-Fickian (Super case II transport)

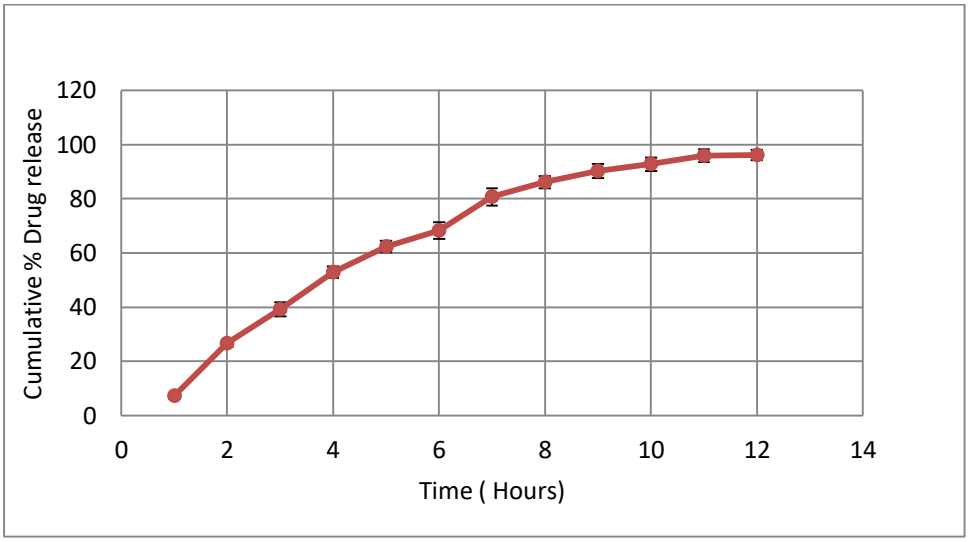

Figure 9: Cumulative % drug release from optimized DXI NE batch

***Ex-vivo skin permeation studies*:**

Analyzing the release of drugs was done using Franz's diffusion cell. An ideal sampling interval was included in the 12-hour experiment. Goat skin was used as the diffusion membrane for the permeation experiments. According to the study for the release, it showed a cumulative medicine percentage of 96.13± 1.92%. According to the drug release study using NEs, the observed transdermal flux was 0.1619 mg/cm^2/hr.

Table 8: Composition of optimized DXI NE gel & conventional gel

Ingredients	**IBU Micellar Gel**	**DXI Micellar Gel**	**DXI NE gel**
API	IBU 5%	DXI 5%	DXI NLC 5%
Methanol	2%	2%	-
Carbopol	1%	1%	1%
Methyl paraben	0.03	0.03	0.03
Propyl paraben	0.01	0.01	0.01
Triethanolamine	q.s.	q.s.	q.s.
Double Distilled Water	q.s.	q.s.	q.s.

Comparative study of optimized carrier incorporated gel with other formulations:

In this study, the experimental outcomes of optimal NE loaded gel formulations were contrasted with those of ideal formulations developed by restricted optimization. According to the experimental findings of the optimized NE and the integrated gel, the gel exhibits nanometric globule size, good entrapment efficiency, high drug release, ex-vivo permeation flux, as well as outstanding handling qualities and simplicity of application.

Table 9: Evaluation of optimized carrier incorporated gel

Evaluation Parameter	**Micellar IBU gel**	**Micellar DXI gel**	**DXI NE Gel**
Globule size (nm)	-	-	122.4
Zeta Potential (mV)	-	-	-0.26
Polydispersity Index	-	-	0.187
Transdermal Flux (µg/ cm2/hr)	-	-	0.2642
Viscosity (cp)	4720	4356	5236
% Drug release	99.61±1.31 (after 6hr.)	99.51±1.16 (after 5hr.)	94.69±2.01 (after 12hr.)
pH	6.0	6.0	6.0
Spreadability gm.cm/s	1.451	1.546	1.442

NE gel that has been optimized for use is compared to micellar DXI gel and micellar IBU gel that has been manufactured without liquid lipid. The batch of optimized NE gel had much superior assessments, pharmacokinetics, and dynamic characteristics (Table 8).

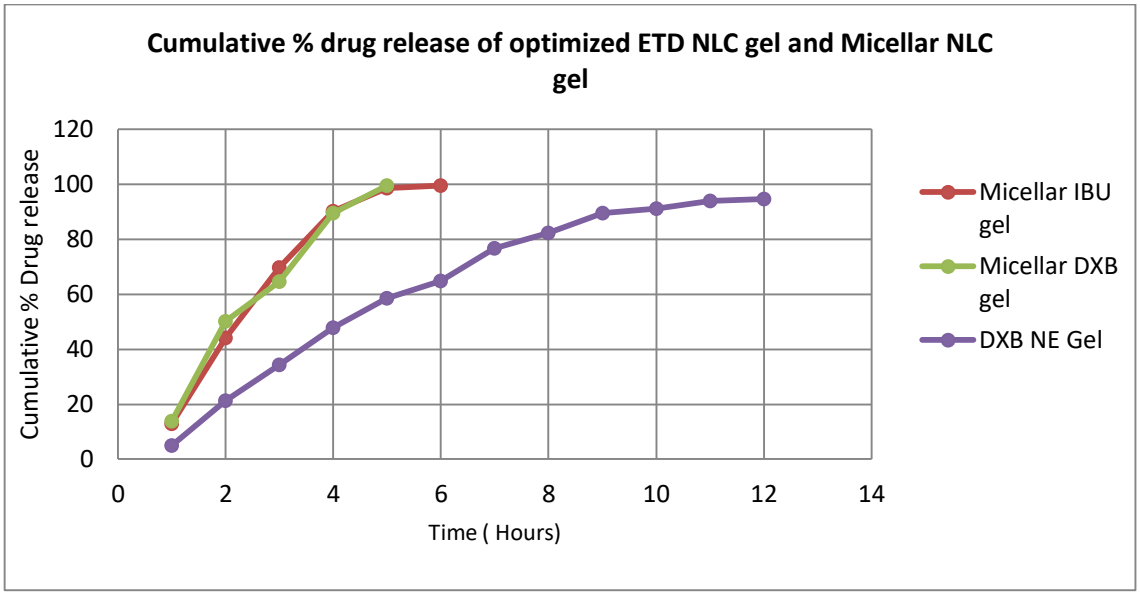

Figure 10: Cumulative % drug release from Micellar IBU gel, Micellar DXI gel and DXI NE gel

Anti-inflammatory activity:

Carrageenan-induced rat paw oedema:

The Institutional Animal Ethical Committee (IAEC) approved the animal testing approach: IAEC/RCPIPER/2021-22/20.

Rats in the control group received treatment with DXI's micellar formulation. IBU loaded micellar gel (group II), DXI loaded micellar gel (group III), and improved NE-based gel formulation of DXI (group IV) were administered to the experimental group, while no topical treatments were given to the control group (group I). Digital caliber was used to take measurements of the foot volume before and after the injection of carrageenan at predetermined intervals. Each group's % inhibition and oedema rate were determined. Increased % inhibition was seen upto 6hr. while oedema treated with DXI NE gel showed activity upto 8-12 hrs.

Figure depicts a graph of percent inhibition against time in hours.

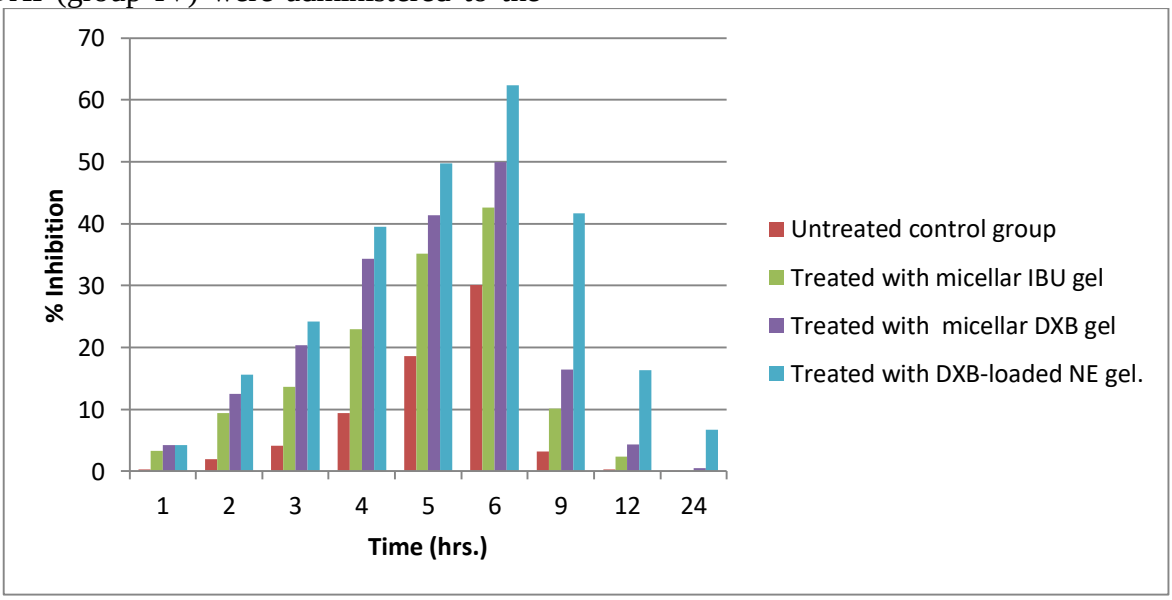

Figure 11: Percent Inhibition graph of Carrageenan-induced rat paw oedema

Anti-nociceptive activity:

Hot plate test: The anti-nociceptive effectiveness of formulations was tested using the hot plate technique, and the results are shown in Figure12. The animal's nociceptive response was timed from the point at which it was put on the hot plate until it showed any response, such as licking its feet, attempting to escape, or elevating its limbs. The investigated formulations demonstrated significant anti-nociceptive effectiveness in comparison to the control groups at almost all time points throughout the experiment. Group IV treated with DXI NE gel had the highest anti-nociceptive effectiveness three hours after the product was applied to the skin. Group III was treated with DXI-loaded micellar gel, which exhibited a much higher anti-nociceptive impact than IBU-loaded micellar gel.

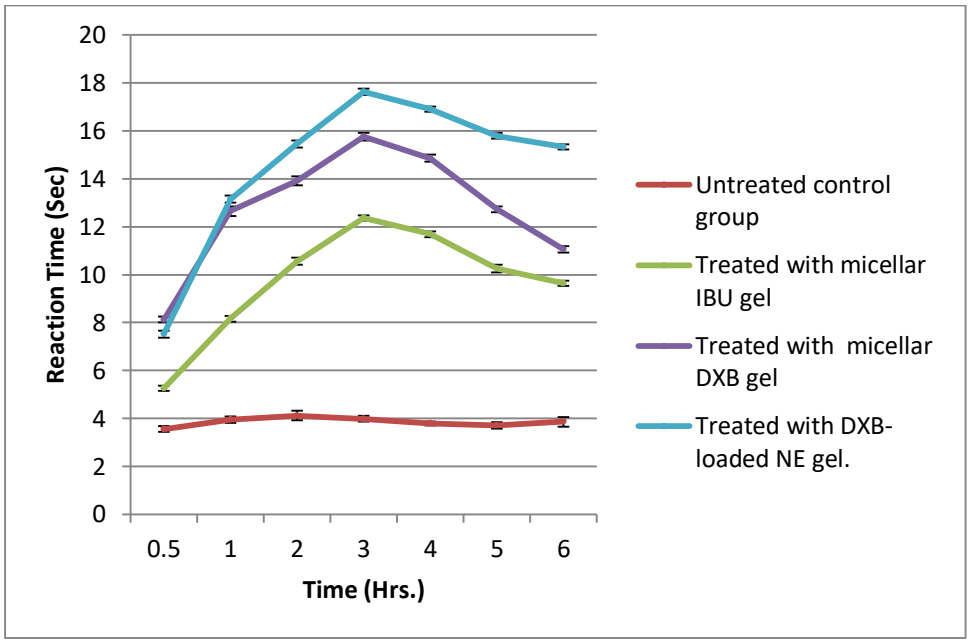

Figure 12: Reaction time of formulations by hot plate method

Stability Studies:

DXI NE gel underwent expedited and long-term stability trials for 3 and 6 months at room temperature and in the refrigerator. Zeta potential, particle size, entrapment effectiveness, and percent drug release of optimized NEs altered hardly at all from baseline values under cold conditions. At ambient temperature, wide changes observed in zeta potential, particle size, entrapment effectiveness, and % drug release. For maximum stability, it is suggested that the NLC formulation be kept chilled. The lipid bilayer's enhanced fluidity at higher temperatures may be the cause of increased leakage.

Table 10: Stability studies of optimized DXI NE

Storage condition / **Sampling Time**	**Accelerated Stability studies 25°C ± 2°C/60% RH ± 5% RH**				**Long term stability studies 4-8°C ± 1°C**			
	Particle Size (nm)	**Zeta potential(mV)**	**Transdermal flux (mg/ cm^2 /hr)**	**Drug release (%)**	**Particle Size (nm)**	**Zeta potential (mV)**	**Transdermal flux (mg/ cm^2 /hr)**	**Drug release (%)**
Initial	122.4	-26.0	0.2262	96.13	122.4	-26.0	0.2262	96.13
After 3months	156.4	-32.06	0.1863	83.14	132.8	-29.21	0.2036	94.54
After 6 months	183.6	-38.14	0.1221	81.20	149.3	-32.0	0.1896	91.96

Discussion:

Using aqueous titration method pseudo ternary phase diagrams were developed based on inference mentioned under methods section for selection of additives. The pseudo-ternary-component phase diagram was used to indicate the NE's zone and stabiity. One axis represented the aqueous phase, the other the oil phase, and the third the mixing of surfactant and co-surfactant at constant volume ratios (Smix ratio). These observations were made independently for each Smix ratio in the group, and phase diagrams were obtained independently for each Smix ratio. The primary criterion was the size of the NE zone as determined by the ternary phase investigation. Based on cosurfactant's capacity to stabilise NE will increase the region of NE [12, 13]. All the cosurfactants are combined with a surfactant in the research at a specific ratio of (Surfactant: co-surfactant 1:2) and each combination analyzed.

Even a phase study was performed utilizing just cosurfactant, labrasol, with no surfactant combinations (0:1). Phase separation was found as a consequence of this composition, which supported the idea that cosurfactant alone cannot function as a stabilising agent but may help to increase the stability of the system dispaying additive effect on surfactant. The stabilisation of the NEs was shown to need a significant quantity of Smix. Thus, through the investigation, we learned that several combinations of 15-20% oil and 40–50% Smix were acceptable for creating NEs. The phase behaviour and NE area of phase diagrams did not change when 5% w/w of DXI was added to the formulations, as was predicted since pH and/or ionic strength had no effect on the production and stability of nano- and microemulsions made up of non-ionic components [30-32].

It was observed that the ratio of the Oil and Smix content had a substantial effect on the mean globule size of different formulations. The size of the globules was found to be smaller with lower oil and higher surfactant concentrations. Additionally, the fact that the PDI values were below 0.3 shows that all NE batches had remarkable homogeneity. While a higher PDI (>0.3) indicates significant particle size heterogeneity, a lower PDI (0.2) suggests a homogenous vesicle population [60-62].

DXI NE formulations developed with Smix (Tween 20: Labrasol) showed improved entrapment efficiency when the Smix content was increased. Smix has a great affinity for the oil surface of the NE and as Smix concentration rises, so does this attraction. At low Smix concentrations, the interaction is weak, resulting in poorer trapping. As when the surfactant concentration was increased, the contact became stronger, resulting in greater entrapment efficiency (Table 3). Surfactant lowers the surface tension of oil drops, allowing them to break down into smaller pieces. Surfactant was present in sufficient amounts to cover the oil droplets' surfaces, stabilising and preventing NE droplet coalescence. The goal was to create a stable NE with a low surfactant content.

The anti-inflammatory and anti-nociceptive result might be explained by the increased surface area of the nanosized formulation, which enhances DXI penetration through the skin's surface and boosts absorption for a stronger anti-nociceptive activity. The effects of DXI and IBU micellar gels were compared in this research to assess therapeutic effectiveness of developed batch, and it was discovered that the dextro form of IBU (DXI) had a quicker response time than the combined form (IBU). This activity may be attributed due to the fact that DXI NE gel exhibit nearly twice potency and quicker than IBU conventional gel.

The drug release pattern of all formulation was found to be linear, zero order, Non-

fickian Supercase-II transport as specified in Korsmeyer peppas model. Tests for both long-term and accelerated stability have an effect on the gel. All parameter beginning and ending values varied significantly under rapid circumstances, however under cold conditions there were less variations.

Conclusion:

In present study DXI NE was prepared using spontaneous nanoemulsification method for improving its solubility and dissolution. Screening of surfactants and cosurfactants studies helped to identify the most suitable excipients, whereas the phase diagrams gave a good idea about the concentrations of the NE components (oil and Smix) that should be employed to achieve nanosized formulations. The pH and drug incorporation studies could differentiate the stability of different compositions and facilitated the selection of most stable formulation.

Anti-inflammatory and anti-nociceptive effect of this formulation was significantly better than micellar IBU and micellar DXI gel that is marketed for anti-inflammatory and anti-arthritic effect. To conclude, NE containing DXI could be introduced as an effective formulation for treatment of inflammation by improving the healing process with reduced dose of conventional dose of IBU. According to the comparative analysis, the improved NE batch outperforms other batches in terms of in-vitro drug release and pharmacological testing. After the drug was released, NEs continued to reduce the percentage of carrageenan-induced rat paw swelling for another 12 hours. For persistent inflammatory diseases like rheumatoid arthritis, the treatment is optimistic. For NE preparations, refrigerated storing is advised to extend expiration life from stability study data.

To identify the therapeutic efficacy of optimized batch on human, clinical studies are recommended. Scalability studies will be needed to ascertain the commercial feasibility. The statistical data shows the potential of controlled and localized drug administration using DXI NE gel is promising.

List of abbreviations:

DEE	=	Drug Entrapment Efficiency
DR	=	Drug Release
IAEC	=	Institutional Animal Ethical Committee
NLC	=	Nanostructured Lipid Carriers
NSAID	=	Nonsteroidal Anti-inflammatory Drug
PBS	=	Phosphate Buffer Solution
PDI	=	Polydispersity Index
SEM	=	Scanning Electron Microscopy
NE	=	Nanormulsion

References:

1. Gaikwad SG, Pandit AB (2008) Ultrasound emulsification: Effect of ultrasonic and physicochemical properties on dispersed phase volume and droplet size. Ultrasonics Sonochemistry 15(40): 554–563. doi:10.1016/j.ultsonch.2007.06.011
2. Nicolas A, Vandamme TF (2009) The universality of low-energy nanoemulsification. International Journal of Pharmacy 377: 142–147.
3. Landfester K, Eisenblätter J, Rothe R (2004) Preparation of polymerizable miniemulsions by ultrasonication. Journal of Coatings Technology and Research 1(1): 65–68. doi:10.1007/s11998-004-0026-y
4. Ghosh V, Saranya S, Mukherjee A, Chandrasekaran N (2013) Cinnamon oil NE formulation by ultrasonic emulsification: Investigation of its bactericidal activity. Journal of Nanoscience and Nanotechnology 13(1): 114–122.

doi:10.1166/jnn.2013.6701

5. Salvia-Trujillo L, Rojas-Graü M A, Soliva-Fortuny R, & Martín-Belloso O (2014) Formulation of antimicrobial edible NEs with pseudo-ternary phase experimental design. Food and Bioprocess Technology 7(10): 3022–3032. doi:10.1007/s11947-014-1314-x
6. Tiwari S, Tan Y M, Amiji M (2006) Preparation and in vitro characterization of multifunctional NEs for simultaneous MR imaging and targeted drug delivery. Journal of Biomedical Nanotechnology 2(3): 217–224. doi:10.1166/jbn.2006.038
7. Behrend O, Ax K, Schubert H (2000) Influence of continuous phase viscosity on emulsification by ultrasound. Ultrasonics Sonochemistry 7(2): 77–85. doi:10.1016/s1350-4177(99)00029-2
8. Borhade VB, Nair HA, Hegde DD (2008) Design and evaluation of selfmicroemulsifying drug delivery system (SMEDDS) of tacrolimus. AAPS PharmSciTech 9(1): 13–21. doi:10.1208/s12249-007-9014-8
9. Pongsumpun, P, Iwamoto S, Siripatrawan U (2020) Response surface methodology for optimization of cinnamon essential oil NE with improved stability and antifungal activity. Ultrasonics Sonochemistry 60: 104604. doi:10.1016/j.ultsonch.2019.05.021
10. Chen ML (2008) Lipid excipients and delivery systems for pharmaceutical development: A regulatory perspective. Advanced Drug Delivery Reviews 60(6): 768–777. doi:10.1016/j.addr.2007.09.010
11. Jatin G, Praveen K (2014) Emerging trends in NE design and therapeutics: A review, Asian Journal of Pharmaceutical Sciences and Clinical Research 2:1–16.
12. Kavitha K, Kanagathara N (2014) Optimization and solubilisation study of novel NE formulation for 5-fluorouracil by applying pseudoternary phase diagram. Asian Journal of Pharmaceutical and Clinical Research 7(2): 137–139.
13. Moreno MA, Ballesteros MP, Frutos P (2003) Lecithin-based oil-in-water microemulsions for parenteral use: Pseudoternary phase diagrams, characterization and toxicity studies. Journal of Pharmaceutical Sciences 92(7): 1428–1437. doi:10.1002/jps.10412
14. Li P, Ghosh A, Krill S, Joshi YM, Serajuddin ATM (2005) Effect of combined use of nonionic surfactant on formation of oil-in-water microemulsions. International Journal of Pharmacy 288: 27–34.
15. Kommuru TR, Gurley B, Khan MA, Reddy IK (2001) Self-emulsifying drug delivery systems (SEDDS) of coenzyme Q10: Formulation development and bioavailability assessment. International Journal of Pharmaceutics 212(2): 233–246. doi:10.1016/s0378-5173(00)00614-1
16. Bachhav YG, Patravale VB (2009) Microemulsion-based vaginal gel of clotrimazole: Formulation, in vitro evaluation, and stability studies. AAPS PharmSciTech 10(2): 476–481. doi:10.1208/s12249-009-9233-2
17. Shakeel F, Baboota S, Ahuja A, Ali J, Aqil M, Shafiq S (2007) NEs as vehicles for transdermal delivery of aceclofenac. AAPS PharmSciTech 8(4): E104. doi:10.1208/pt0804104
18. Gohel M, Soni T, Hingorani L, Patel A, Patel N (2014) Development and optimization of plant extract loaded NE mixtures for the treatment of inflammatory disorder. Current Research in Drug Discovery 1(2): 29–38. doi:10.3844/crddsp.2014.29.38

19. Hussain A, Samad A, Singh SK, Ahsan MN, Haque MW, Faruk A, Ahmed FJ (2016) NE gel-based topical delivery of an antifungal drug: In-vitro activity and in-vivo evaluation. Drug Delivery 23(2): 642–647. doi:10.3109/10717544.2014.933284
20. Zhu S, Hong M, Liu C, Pei Y (2009) Application of box-Behnken design in understanding the quality of genistein self-nanoemulsified drug delivery systems and optimizing its formulation. Pharmaceutical Development and Technology 14(6): 642–649. doi:10.3109/10837450902882385
21. Kaur A, Katiyar SS, Kushwah V, Jain S (2017) NE loaded gel for topical co-delivery of clobitasol propionate and calcipotriol in psoriasis. Nanomedicine: Nanotechnology, Biology, and Medicine 13(4): 1473–1482. doi:10.1016/j.nano.2017.02.009
22. Ferreira SLC, Bruns RE, Ferreira HS, Matos GD, David JM, Brandão GC, Santos WN (2007) Box-Behnken design: An alternative for the optimization of analytical methods. Analytica Chimica Acta 597(2): 179–186. doi:10.1016/j.aca.2007.07.011
23. Patel N, Thakkar V, Moradiya P, Gandhi T, Gohel M (2015) Optimization of curcumin loaded vaginal in-situ hydrogel by box-Behnken statistical design for contraception. Journal of Drug Delivery Science and Technology 29: 55–69. doi:10.1016/j.jddst.2015.06.002
24. Zhu S, Hong M, Liu C, Pei Y (2009) Application of box-Behnken design in understanding the quality of genistein self-nanoemulsified drug delivery systems and optimizing its formulation. Pharmaceutical Development and Technology 14(6): 642–649. doi:10.3109/10837450902882385
25. Shafiq-un-Nabi S, Shakeel F, Talegaonkar S, Ali J, Baboota S, Ahuja A, Ali M (2007) Formulation development and optimization using NE technique: A technical note. AAPS PharmSciTech 8(2): Article 28. doi:10.1208/pt0802028
26. Makhmalzadeh BS, Torabi S, Azarpanah A (2012) Optimization of ibuprofen delivery through rat skin from traditional and novel NE formulations. Iranian journal of pharmaceutical research: IJPR 11(1): 47.
27. Patel RP, Joshi JR (2012) An overview on NE: A novel approach. International Journal of Pharmaceutical Sciences and Research 3(12): 4640.
28. Anton N, Vandamme TF (2011) NEs and microemulsions: Clarifications of the critical differences. Pharmaceutical Research 28(5): 978–985. doi:10.1007/s11095-010-0309-1
29. Date AA, Desai N, Dixit R, Nagarsenker M(2010) Self-nanoemulsifying drug delivery systems: Formulation insights, applications and advances. Nanomedicine 5(10): 1595–1616. doi:10.2217/nnm.10.126
30. Mahdi ZH, Maraie NK (2019) Overview on NE as a recently developed approach in Drug nanoformulation. Research Journal of Pharmacy and Technology 12(11): 5554–5560. doi:10.5958/0974-360X.2019.00963.6
31. Lawrenc MJ, Rees GD (2000) Microemulsion-based media as novel drug delivery systems. Advanced Drug Delivery Reviews 45(1): 89–121. doi:10.1016/S0169-409X(00)00103-4

32. Tenjarla S (1999) Microemulsions: An overview and pharmaceutical applications. Critical Reviews in Therapeutic Drug Carrier Systems 16(5): 461–521. doi:10.1615/CritRevTherDrugCarrierSyst.v16.i5.20

33. Ghosh PK, Murthy RS (2006) Microemulsions: A potential drug delivery system. Current Drug Delivery 3(2): 167–180. doi:10.2174/156720106776359168

34. Shafiq S, Shakeel F, Talegaonkar S, Ahmad FJ, Khar RK, Ali M (2007) Development and bioavailability assessment of ramipril NE formulation. European Journal of Pharmaceutics and Biopharmaceutics 66(2): 227–243. doi:10.1016/j.ejpb.2006.10.014

35. Ali MS, Alam MS, Alam N, Siddiqui MR (2014) Preparation, characterization and stability study of dutasteride loaded NE for treatment of benign prostatic hypertrophy. Iranian Journal of Pharmaceutical Research 13(4): 1125–1140.

36. Azeem A, Rizwan M, Ahmad FJ, Iqbal Z, Khar RK, Aqil M, Talegaonkar S (2009) NE components screening and selection: A technical note. AAPS PharmSciTech 10(1): 69–76. doi:10.1208/s12249-008-9178-x

37. Jaiswal M, Dudhe R, Sharma PK (2015) NE: An advanced mode of drug delivery system. Biotech 5(2): 123–127. doi:10.1007/s13205-014-0214-0

38. Domalapally S, Revathi AI, Jaya S, Teja, ND (2014) Enhancement of dissolution profile of poorly water soluble drug (nimodipine) by using liquisolid compact technique. International Journal of Pharmaceutical Sciences 4(1): 447–456.

39. Shaker DS, Ishak RAH, Ghoneim A, Elhuoni MA (2019) NE: A review on mechanisms for the transdermal delivery of hydrophobic and hydrophilic drugs. Scientia Pharmaceutica 87(3): 17. doi:10.3390/scipharm87030017

40. Sharma A, Singh AP, Harikumar SL (2020) Development and optimization of NE based gel for enhanced transdermal delivery of nitrendipine using box-Behnken statistical design. Drug Development and Industrial Pharmacy 46(2): 329–342. doi:10.1080/03639045.2020.1721527

41. Kumbhar SA, Kokare CR, Shrivastava B, Gorain B, Choudhury, H (2020) Preparation, characterization, and optimization of asenapine maleate mucoadhesive NE using Box-Behnken design: In vitro and in vivo studies for brain targeting. International Journal of Pharmaceutics 586: 119499. doi:10.1016/j.ijpharm.2020.119499

42. Aqil M, Kamran M, Ahad A, Imam SS (2016) Development of clove oil based NE of olmesartan for transdermal delivery: Box–Behnken design optimization and pharmacokinetic evaluation. Journal of Molecular Liquids 214: 238–248. doi:10.1016/j.molliq.2015.12.077

43. Tortora GJ, Grabowski SR (1996) Principle of Anatomy and physiology (10th ed). Harpercolins College Publishers.

44. Pena LE, Osborne DW, Amann AH (1990) Topical drug delivery formulation. New York: Marcel Dekker 381–388.

45. Phillips CR, Brasington RD (2010) Osteoarthritis treatment update: Are NSAIDs still in the picture. Journal of Musculoskeletal Medicine 27(2).

46. Sharma A, Saini S, Rana A (2013) Transdermal drug delivery system: A review. International Journal of

Research in Pharmaceutical and Biomedical Sciences 4: 286–292.

47. Rastogi V, Yadav P (2012) Transdermal drug delivery system: An overview. Asian Journal of Pharmaceutics 6(3): 161–170. doi:10.4103/0973-8398.104828
48. Langer R (2004) Transdermal drug delivery: Past progress, current status, and future prospects. Advanced Drug Delivery Reviews 56(5): 557–558. doi:10.1016/j.addr.2003.10.021
49. Waugh A, Grant A (2006) Ross and Wilson Anatomy and Physiology in health and illness (10th ed). New York: Churchill Livingstone.
50. Shakeel F, Ramadan W, Ahmed MA (2009) Investigation of true NEs for transdermal potential of indomethacin: Characterization, rheological characteristics, and ex vivo skin permeation studies. Journal of Drug Targeting 17(6): 435–441. doi:10.1080/10611860902963021
51. Thomas L, Zakir F, Mirza MA, Anwer MK, Ahmad FJ, Iqbal Z (2017) Development of curcumin loaded chitosan polymer based NE gel: In vitro, ex vivo evaluation and in vivo wound healing studies. International Journal of Biological Macromolecules 101: 569–579. doi:10.1016/j.ijbiomac.2017.03.066
52. Ahmad N, Ahmad R, Mohammed Buheazaha T, Salman AlHomoud H, Al-Nasif HA, Sarafroz M (2020) A comparative ex vivo permeation evaluation of a novel 5-Fluorocuracil NE-gel by topically applied in the different excised rat, goat, and cow skin. Saudi Journal of Biological Sciences 27(4): 1024–1040. doi:10.1016/j.sjbs.2020.02.014
53. Razzaq FA, Asif M, Asghar S, Iqbal MS, Khan IU, Khan SU (2021) Glimepiride-loaded nanoemulgel; development, in vitro characterization, ex vivo permeation and in vivo antidiabetic evaluation. Cells 10(9): 2404. doi:10.3390/cells10092404
54. Botros SR, Hussein AK, Mansour HF (2020) A novel NE intermediate gel as a promising approach for delivery of itraconazole: Design, in vitro and ex vivo appraisal. AAPS PharmSciTech 21(7): 272. doi:10.1208/s12249-020-01830-w
55. Joshi M, Patravale V (2008) Nanostructured lipid carrier (NLC) based gel of celecoxib. International Journal of Pharmaceutics 346(1–2): 124–132. doi:10.1016/j.ijpharm.2007.05.060
56. Esmaeili F, Zahmatkeshan M, Yousefpoor Y, Alipanah H, Safari E, Osanloo M (2022) Anti-inflammatory and anti-nociceptive effects of Cinnamon and Clove essential oils nanogels: An in vivo study. BMC Complementary Medicine and Therapies 22(1): 143. doi:10.1186/s12906-022-03619-9
57. Braroo P, Bajaj A, Jain D, Maskare R, Babul N, Kao H (2013) Anti-inflammatory and anti-nociceptive activity of nanogels containing naproxen. Journal of Pain 14(4), Suppl. 86. doi:10.1016/j.jpain.2013.01.681
58. Abdallah MH, Abu Lila AS, Unissa R, Elsewedy HS, Elghamry HA, Soliman MS (2021) Preparation, characterization and evaluation of anti-inflammatory and anti-nociceptive effects of brucine-loaded nanoemulgel. Colloids and Surfaces. B, Biointerfaces 205: 111868. doi:10.1016/j.colsurfb.2021.111868
59. Ali MS, Alam MS, Alam N, Siddiqui MR (2014) Preparation, characterization and stability study of dutasteride loaded NE for treatment of benign prostatic hypertrophy. Iranian Journal of Pharmaceutical Research 13(4): 1125–1140.

60. Wulansari A, Jufri M, Budianti A (2017) Studies on the formulation, physical stability, and in vitro antibacterial activity of tea tree oil (Melaleuca alternifolia) NE gel. International Journal of Applied Pharmaceutics 9(1): 135–139. doi:10.22159/ijap.2017.v9s1.73_80

61. Elmowafy M, Samy A, Raslan, MA, Salama A, Said RA, Abdelaziz AE, Viitala T (2016) Enhancement of bioavailability and pharmacodynamic effects of thymoquinone via nanostructured lipid carrier (NLC) formulation. AAPS PharmSciTech 17(3): 663–672. doi:10.1208/s12249-015-0391-0

62. Kitimu SR, Kirira P, Sokei J, Ochwangi D, Mwitari P, Maina N(2022) Biogenic synthesis of silver nanoparticles using Azadirachta indica methanolic bark extract and their anti-proliferative activities against DU-145 human prostate cancer cells. African Journal of Biotechnology 21(2): 64–72.